ITS-90 CALIBRATION OF RADIATION THERMOMETERS FOR RTP USING WIRE/THIN-FILM THERMOCOUPLES ON A WAFER

C.W. Meyer, D.P. DeWitt, K.G. Kreider, F.J. Lovas, and B.K. Tsai

National Institute of Standards and Technology
Gaithersburg, MD 20899

Abstract. Light-pipe radiation thermometers (LPRTs) are the sensor system of choice in RTP tools. They can be calibrated against blackbodies with an uncertainty (k=1) less than 0.3 °C. In an RTP tool, however, account must be made for wafer emissivity and wafer-chamber interreflections, or else temperature measurement uncertainties will be orders of magnitude higher. We have used two complementary approaches for accomplishing this: 1) *in situ* calibration using high-accuracy wire/thin-film thermocouples calibrated on the International Temperature Scale of 1990 (ITS-90) and 2) developing optical models to estimate the effective emissivity of the wafer ε_{eff} when used in the radiation environment of the RTP tool. The temperature measurement uncertainty of LPRTs using either technique is 2.1 °C or less.

INTRODUCTION

Accurate temperature measurement of silicon wafers during rapid thermal processing (RTP) is of critical importance for manufacturing reliable, high quality devices. To meet the Semiconductor Industry Association roadmap requirements, RTP temperature measurement accuracy of better than 2 °C and temperature measurement reproducibility of better than 0.25 °C at 1000 °C are needed [1]. Light-pipe radiation thermometers (LPRTs) are the sensor system of choice in RTP tools because of their small size and minimum thermal disturbance of the heated wafer. LPRTs can be calibrated against blackbodies with an uncertainty less than 0.3 °C [2] (all uncertainties referred to here have a coverage factor of $k = 1$). In an RTP tool, however, account must be made for wafer emissivity and wafer-chamber interreflections, or else temperature measurement uncertainties will be orders of magnitude higher [3,4]. We have used two complementary approaches for accomplishing this. The first is to perform *in situ* calibration of LPRTs in the RTP tool [5] using wire/thin-film thermocouples (TCs) [6,7] calibrated on the International Temperature Scale of 1990 (ITS-90) [8]. The TCs have a temperature measurement uncertainty of less than 0.4 °C [6]. Temperature measurements using the *in situ* calibration are referred to as T_{iscal}. The second approach is to develop optical models to estimate the effective emissivity of the wafer ε_{eff} when used in the radiation environment of the RTP tool [9,10]. Knowing ε_{eff}, the wafer temperature T can be calculated from the indicated spectral radiance temperature T_λ measured by a blackbody-calibrated LPRT using the temperature measurement equation [10],

$$\frac{1}{T} = \frac{1}{T_\lambda} + \frac{\lambda}{c_2} \cdot \ln \varepsilon_{eff} , \tag{1}$$

where λ is the wavelength and c_2 is the second radiation constant. Temperatures determined in this way are designated as T_{mod}.

In this paper we present results of steady-state measurements of T_{iscal} and T_{mod} on silicon wafers in our RTP test bed tool over the temperature range 650 °C to 920 °C. In the test bed, the cavity underneath the wafer is surrounded with shields of high reflectivity that minimize stray lamp irradiation and enhance wafer-shield interreflections that raise significantly the effective emissivity of the wafer surface. The optical environment (i.e. ε_{eff}) can be altered by changing the reflectance of the bottom shield and/or the spacing between the wafer and bottom shield. The ability to change these parameters allows evaluation of the robustness of the effective emissivity models to account for environment features as well as maximize ε_{eff}. The models have included influences of shield reflectivity, wafer emissivity, wafer-shield gap separation distance and light-pipe sensing tip diameter [9]. These models can be validated by comparison of T_{mod} with T_{iscal}.

WAFER AND RTP TOOL

Figure 1 shows the design of the 200-mm thermocouple-instrumented wafer, which is described in greater detail in [6,7]. The wafer had four rhodium-platinum thin-film thermocouples (TFTCs). The four junctions were labeled 7, 9, 10, and 12 as shown. TFTCs 7 and 9 measured the temperature difference between their junctions and weld pad 8. Similarly, TFTCs 10 and 12 measured the temperature difference between their junctions and weld pad 11. Temperatures at weld pads 8 and 11 were measured with Pt/Pd wire thermocouples. Only those measurements made with junction 10 are presented in this paper. The LPRT targets, which also are shown in Fig. 1, are labeled 1, 3 and 4. Target 1 is separated from TFTC junctions 9 and 10 by 1.6 cm in order to avoid affecting the emissivity of the wafer over the LPRT target area.

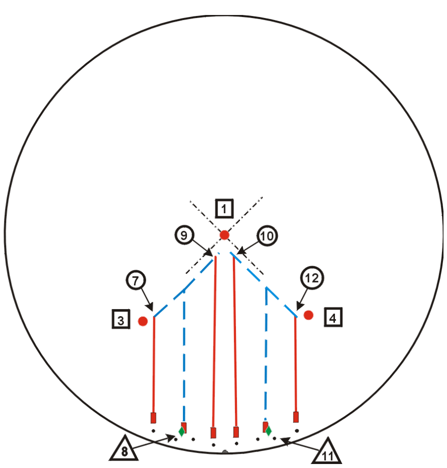

The NIST RTP test bed is shown in Figure 2 and is described in detail in [5]. The walls were made of stainless steel and the top of the test bed was composed of a quartz plate. The test bed was purged with pure nitrogen gas. Heating was produced by quartz-halogen lamps located above the test bed. The calibration wafer was located below the quartz plate as shown. A silicon shading wafer was placed directly above the calibration wafer to compensate for nonuniformities in radiative heating from the lamps; with this arrangement, temperature variations on the calibration wafer were less than 9 °C.

FIGURE 1. NIST thermocouple-instrumented wafer. The Pt thin films are shown as solid lines and the Rh thin films are shown as dashed lines. Labels 1, 3, and 4 represent LPRT targets. Labels 8 and 11 represent Pt/Pd wire thermocouple junctions. Labels 7, 9, 10, and 12 represent Rh/Pt thin-film thermocouple junctions.

Underneath the wafer was a water-cooled copper plate. Atop the plate was a reflective shield, which was held tight against the plate by a vacuum. Two gold-coated reflective shields were made for use with the RTP test bed; one providing diffuse reflection and the other providing specular reflection. From total hemispherical reflectance measurements, the reflectance of the diffuse shield was ρ = 0.799, and that of the specular shield was ρ = 0.993. Five holes were drilled through the copper plate and shield to allow for insertion of LPRTs. One hole was in the center of the plate and the other four were located at a radius of 5.4 cm from the center of the plate and at equal angles from each other. In addition, three holes were drilled through the copper plate and reflective

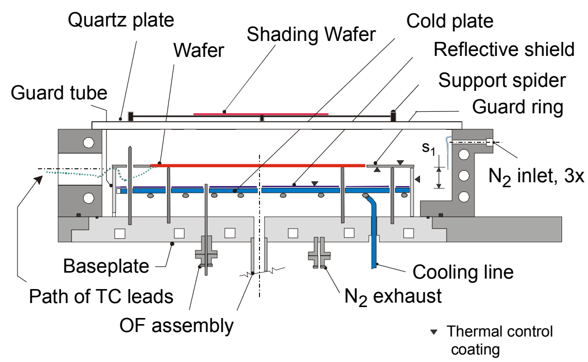

shields at equal angles to allow for the insertion of the alumina rods supporting the wafer.

The copper plate was surrounded by a platinum-coated quartz guard tube as shown in the figure. On top of the guard tube rested a platinum-coated quartz guard ring as shown. This design provided an enclosure underneath the wafer that was almost completely shielded from stray radiation and which was surrounded on the top and sides by platinum-coated reflective shields and on the bottom by a gold-coated reflective shield. By supporting the wafer with sets of rods of different length, the spacing between the wafer and the bottom reflective shield could be adjusted.

The LPRTs used were commercially made and consisted of three 2-mm diameter sapphire light pipes connected with optical fibers to a radiometer. The light pipes were surrounded by sapphire sheaths of 3.8 mm outer diameter. They were calibrated at NIST against a sodium heat-pipe blackbody source [2] and

FIGURE 2. The NIST RTP Test Bed.

then placed in the RTP test bed such that their tips were flush with the top of the reflective shield.

The measurement procedure is described in greater detail in [5]. The emf across each thermocouple was measured with a high-accuracy multimeter. Data acquisition was automated by a personal computer interfaced with the LPRTs, scanner and multimeter. Measurements of contact temperature (using thermocouples) and of spectral radiance temperature (using LPRTs) were made under steady heating at various power levels. Wafer temperatures ranged between 650 °C and 920 °C. Measurements were performed using both diffuse and specular shields. Four different wafer/shield spacings were used.

EMISSIVITY MODELS

The models developed for calculating the effective emissivity of the wafer have been described in detail in [9]. In brief, the models featured five zones (shown in Figure 3) surrounding the enclosure underneath the wafer. They were (1) the light pipe (assumed to be cold and black); (2) the reflective shield; (3) the guard tube and guard ring (assumed to be cold and, for simplicity, black); (4) the spot on the wafer corresponding to the field-of-view of the light pipe on the wafer, (which had the same characteristics as the rest of the wafer); and (5) the wafer (assumed to emit and reflect diffusely and have a uniform temperature). Two types of cold reflective shields were modeled: a diffuse shield with a reflectance of 0.799 and a specular shield with a reflectance of 0.993. In both models, the remaining surfaces in the enclosure were diffuse. Both models allowed the spacing between the wafer and shield to vary from 6 mm to 12.5 mm. The spectral emissivity (at 0.955 μm) was assumed to be that for bare silicon with a slight temperature dependence according to the empirical relation:
$\varepsilon_\lambda = 0.691 - 5\times10^{-5}\times T/°C$ [9].

For the diffuse shield, the enclosure model was

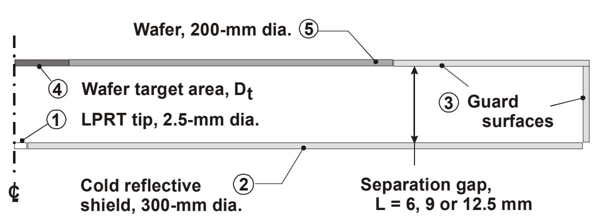

developed using the classical radiosity method [11], and so a radiation energy balance was written for each zone of the 5-zone enclosure. For the specular shield,

FIGURE 3. Cross-section schematic of the enclosure underneath the wafer in the NIST RTP test bed, showing the five zones used in the effective emissivity models.

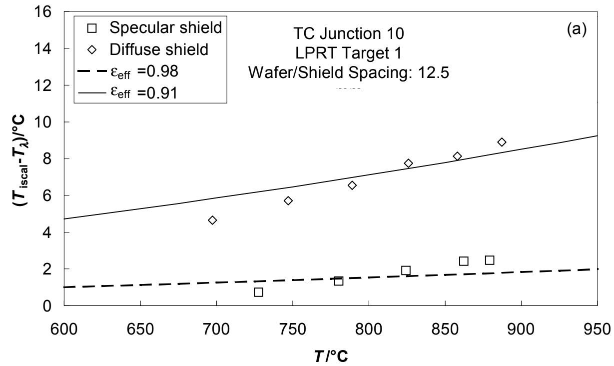

the classical radiation transfer enclosure analysis model for specular and diffuse surfaces was implemented [11]. In this model, the specular surfaces reflected specularly and the diffuse surfaces reflected diffusely, but all surfaces of the enclosure emitted diffusely.

UNCERTAINTIES

The *in situ* calibration involves measuring the difference between the display temperature of the LPRT and the contact temperature measured by the wire/thin-film thermocouple combination. This difference is then used as a correction to the LPRT display temperature at later times to obtain the wafer temperature T_{iscal}. When the blackbody calibration is used, effective emissivity values from the emissivity models are used with the spectral radiance temperatures measured by the LPRTs and with Eq. 1 to obtain the wafer temperature T_{mod}.

Uncertainty discussions here are based on the ISO guidelines for the evaluation of uncertainties [12]. The uncertainties for T_{iscal} and T_{mod} are given below in Table 1. The coverage factor for the uncertainties is k=1. Uncertainty totals are calculated by adding their components in quadrature.

For T_{iscal}, the dominant uncertainty arises from the separation between the thin-film thermocouple junctions and the center of the LPRT target. The uncertainty estimate of 2.0 °C was based on a linear extrapolation of the gradient observed between junction 12 and junction 10. Other measurement uncertainties were from temperature fluctuations and long-term temperature drift of the wafer while in steady state, thermocouple calibration uncertainties, LPRT calibration uncertainties, and instrument uncertainties for temperature measurement with the thermocouples and LPRTs.

For T_{mod}, the dominant uncertainty arises from the calculation of the effective emissivity. This is due to uncertainty in the assumptions made by the model about the experimental system. The other major uncertainty in T_{mod} is due to LPRT blackbody calibration uncertainties.

TABLE 1. Uncertainties (k = 1) for T_{iscal} and T_{mod}

(Uncertainty of T_{iscal})/°C		**(Uncertainty of T_{mod})/°C**	
Pd/Pt TC Calibration	0.1	BB Calibration	0.2
TFTC Calibration	0.3	LPRT display	0.1
TC emf	0.1	Effective emissivity	2.0
LPRT display	0.1		
Temperature drift and fluctuations	0.4		
Junction/target temp difference	2.0		
Total	2.1	Total	2.0

RESULTS

Figure 4a shows a comparison of T_{iscal} and T_{λ} using LPRT target 1 and TFTC junction 10 and with a wafer/shield spacing of 12.5 mm. The uncertainty of $T_{iscal} - T_{\lambda}$ is essentially that of T_{iscal}. Results using the diffuse shield and specular shield are shown as diamonds and squares, respectively. The values of $T_{iscal} - T_{\lambda}$ for the specular shield are all within 2.5 °C ± 2.1 °C. Without the cold reflective shields, T_{λ} can differ from T_{iscal} by more than 25 °C at 900 °C. The values of $T_{iscal} - T_{\lambda}$ for the diffuse shield are larger. This is expected, because the reflectance of the diffuse shield is lower, and so its value for ε_{eff} is expected to be smaller [9]. The curves shown represent the temperature difference expected for effective emissivities of 0.91 and 0.98 calculated using Eq. 1. The emissivity values were chosen so that the curves would best fit the data. The slope of the data in Fig. 4a is clearly larger than that of the curves, showing that ε_{eff} for the wafer decreases with temperature.

Figure 4b shows the effects on $T_{iscal} - T_{\lambda}$ of changing the wafer/shield spacing. For this plot, the specular shield was used. While the results for spacings of 12.5 mm and 15.5 mm are identical to within the resolution of the measurements, the values for $T_{iscal} - T_{\lambda}$ increase as the spacing is decreased from 12.5 mm to 6 mm. This effect can be explained by the optical perturbation on ε_{eff} of the LPRT target area caused by the presence of the light pipe, which has a much smaller reflectance (ρ = 0.075) than the shield. The light pipe occupies a larger solid angle of the field-of-view of a point on the target area as the wafer/shield spacing decreases. Because of this effect, an *in situ* calibration should be performed with the same spacing as in the application.

The difference between T_{iscal} and T_{mod} is shown in Figure 5 as a function of wafer temperature for a wafer/shield spacing of 12.5 mm. For the specular shield, the difference amounts to about 1.3 °C, centered about zero difference, but with an appreciable positive, near-linear trend. Overall, the agreement is within ± 0.6 °C. For the diffuse shield, the difference

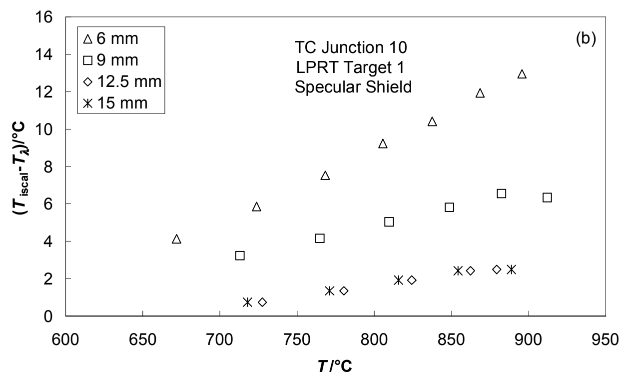

trends are similar, but T_{mod} is systematically higher than T_{iscal} by about 2 °C. The disagreement between the values of $T_{iscal} - T_{mod}$ for the specular and diffuse shields is less than the uncertainty of T_{mod}. Furthermore, the plot shows that T_{iscal} and T_{mod} agree with each other to within their combined uncertainties. It is hoped that future improvements on the models to make them more realistic will lower the uncertainty of T_{mod}. Also, decreasing the separation between the thin-film thermocouple junctions and the LPRT targets on the wafer should lower the uncertainty of T_{iscal}.

SUMMARY

We performed *in situ* calibrations of LPRTs in an RTP test bed against wire/thin-film thermocouple combinations calibrated on the ITS-90. The test bed was designed with cold reflective shields that blocked stray radiation and increased the effective emissivity of the wafer. Calibrations to determine T_{iscal} were performed with an uncertainty (k=1) of 2.1 °C. When the optimal test bed configuration was used, values of

FIGURE 4. Difference between wafer temperature measured using an LPRT with an *in situ* calibration (T_{iscal}) and with no correction to the spectral radiance temperature (T_{λ}). The temperatures were measured near the center of the wafer. In (a) the wafer/shield spacing is 12.5 mm and the results with a gold specular shield (reflectance ρ = 0.993) and a gold diffuse shield (ρ = 0.799) are shown. The curves show the values that would be expected for effective emissivities of 0.91 and 0.98 using Eq. 1. In (b) the specular shield is used, and results with four different wafer/shield spacings are shown.

T_λ agreed with values of T_{iscal} to within 2.5 °C; this corresponded to an effective emissivity of $\varepsilon_{eff} \approx 0.98$. Without the cold reflective shields, T_λ can differ from T_{iscal} by more than 25 °C at 900 °C. We also developed models to determine the effective emissivity of the wafer when used in the RTP test bed. With the model-determined ε_{eff}, we could correct T_λ to obtain T_{mod} with an uncertainty of 2.0 °C. T_{iscal} and

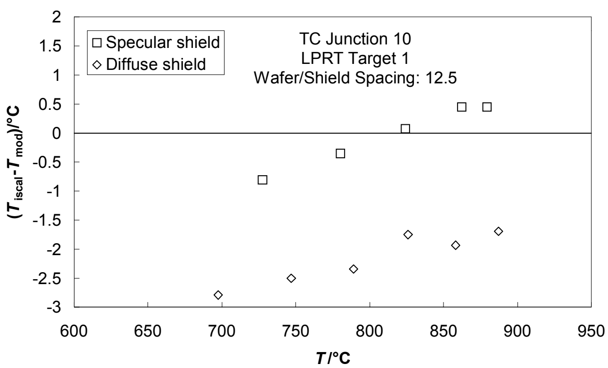

FIGURE 5. Comparisons between T_{iscal} and temperatures measured by an LPRT and corrected using the five-zone emissivity model (T_{mod}). The data is that used in Figure 4(a).

T_{mod} agreed with each other to within 3.0 °C, which was within their combined uncertainties. It is hoped that improvements in the thin-film design on the wafer and in the models will lower the uncertainties significantly.

REFERENCES

1. SIA Semiconductor Industry Association, The National Technology Roadmap for Semiconductors, 3rd edition, Semiconductor Industry Association, San Jose, 1997.

2. Lovas F.J., Tsai B.K., Gibson C.E., "Meeting RTP Temperature Accuracy Requirements: Measurement and Calibrations at NIST", Mat. Res. Soc. Proc., vol. 525, edited by _zturk et.al., MRS 1998, pp. 127-133.

3. DeWitt D.P., Sorrell F.Y., Elliott J.K., "Temperature Measurement Issues in Rapid Thermal Processing", Mat. Res. Soc. Proc., vol. 470, edited by Riley et. al., MRS 1997, pp. 3-15.

4. Adams B.E., "The Challenges of Temperature Measurement in the Semiconductor Industry" in Proceedings of TEMPMEKO ‹99, edited by J.F. Dubbeldam and M.J. deGroot, Delft: NMi Van Swinden Laboratorium, 1999, pp. 3-10.

5. Meyer, C.W., Allen D.W., DeWitt, D.P., Kreider K.G., Lovas F.J., Tsai, B.K., "ITS-90 Calibration of Radiometers Using Wire/Thin-film Thermocouples in the NIST RTP Tool: Experimental Procedures and Results", in Proc. RTP '99, edited by H. Kitayama et. al., Colorado Springs, CO: RTP-Conference, 1999, pp. 136-141.

6. Kreider K.G., DeWitt D.P., Tsai B.K., Lovas F.J., Allen, D.W., "Calibration Wafer for Temperature Measurements in RTP Tools", in Proceedings of the 1998 International Conference on Characterization and Metrology for ULSI Technology, edited by D.G. Seiler et. al., New York: AIP, 1998, pp. 303-309.

7. Kreider K.G., Gillen, G., "Thin-film Calibration Wafer Materials for RTP Temperature Measurement", in Proc. RTP '99, edited by H. Kitayama et. al., Colorado Springs, CO: RTP-Conference, 1999, pp. 142-147.

8. Preston-Thomas H., *Metrologia* **27,** 3-10, 107 (1990).

9. Tsai, B.K., DeWitt, D.P., "ITS-90 Calibration of Radiometers Using Wire/Thin-film Thermocouples in the NIST RTP Tool: Effective Emissivity Modeling", in Proc. RTP '99, edited by H. Kitayama et. al., Colorado Springs, CO: RTP-Conference, 1999, pp. 125-135.

10. DeWitt D.P., Nutter G.D., *Theory & Practice of Radiation Thermometry*, 1st edition, New York: John Wiley & Sons, Inc., 1988.

11. Siegel R., Howell J.R., *Thermal Radiation Heat Transfer*, Washington: Hemisphere Publishing Corporation, 1992.

12. ISO, *Guide to the Expression of Uncertainty in Measurement,* Geneva, Switzerland: International Organization for Standardization, 1993.